

Title	Optimization of diaryl amine derivatives as kinesin spindle protein inhibitors.
Author(s)	Takeuchi, Tomoki; Oishi, Shinya; Kaneda, Masato; Misu, Ryosuke; Ohno, Hiroaki; Sawada, Jun-ichi; Asai, Akira; Nakamura, Shinya; Nakanishi, Isao; Fujii, Nobutaka
Citation	Bioorganic & medicinal chemistry (2014), 22(12): 3171-3179
Issue Date	2014-06-15
URL	http://hdl.handle.net/2433/189466
Right	© 2014 Elsevier Ltd.
Type	Journal Article
Textversion	author

Optimization of Diaryl Amine Derivatives as Kinesin Spindle Protein Inhibitors

Tomoki Takeuchi^a, Shinya Oishi^{a,*}, Masato Kaneda^a, Ryosuke Misu^a, Hiroaki Ohno^a, Jun-ichi Sawada^b, Akira Asai^b, Shinya Nakamura^c, Isao Nakanishi^c, Nobutaka Fujii^{a,*}

^aGraduate School of Pharmaceutical Sciences, Kyoto University, Sakyo-ku, Kyoto 606-8501, Japan

^bGraduate School of Pharmaceutical Sciences, University of Shizuoka, Suruga-ku, Shizuoka 422-8526, Japan

^cFaculty of Pharmacy, Kinki University, 3-4-1 Kowakae, Higashi-osaka 577-8502, Japan

Corresponding Authors:

Shinya Oishi, Ph.D. and Nobutaka Fujii, Ph.D.

Graduate School of Pharmaceutical Sciences

Kyoto University

Sakyo-ku, Kyoto, 606-8501, Japan

Tel: +81-75-753-4551; Fax: +81-75-753-4570,

E-mail (S.O.): soishi@pharm.kyoto-u.ac.jp; E-mail (N.F.): nfujii@pharm.kyoto-u.ac.jp

Abstract

Structure–activity relationship studies of diaryl amine-type KSP inhibitors were carried out. Diaryl amine derivatives with a pyridine ring or urea group were less active when compared with the parent carboline and carbazole derivatives. Optimization studies of a lactam-fused diphenylamine-type KSP inhibitor revealed that the aniline NH group and 3-CF₃ phenyl group were indispensable for potent KSP inhibition. Modification with a seven-membered lactam-fused phenyl group and a 4-(trifluoromethyl)pyridin-2-yl group improved aqueous solubility while maintaining potent KSP inhibitory activity. From these studies, we identified novel diaryl amine-type KSP inhibitors with a favorable balance of potency and solubility.

Keywords: diaryl amine, kinesin spindle protein, aqueous solubility

1. Introduction

Kinesins constitute a superfamily of molecular motor proteins to move along microtubules.¹ Mitotic kinesins are involved in cell division.² Non-mitotic kinesins are principally involved in intracellular transport of organelles and vesicles.³ The kinesin spindle protein (KSP; also known as Eg5) is the mitotic kinesin that belongs to the kinesin-5 family. The structure of KSP is comprised of three parts: an N-terminal motor domain, a central α -helical coiled coil stalk domain, and a C-terminal tail domain.⁴ The N-terminal motor domain contains a catalytic site for ATP hydrolysis and microtubule binding region. KSP moves toward the plus end of the microtubule, just like other kinesins with an N-terminal motor domain, using the energy generated from the hydrolysis of ATP.⁵ The KSP movement is required for centrosome separation and bipolar spindle formation during cell division. Inhibition of KSP leads to mitotic arrest in the prometaphase with the formation of the monopolar spindle and subsequent apoptotic cell death.⁶⁻⁹ Therefore, KSP inhibitors are

expected to be favorable agents for cancer chemotherapy without neurotoxic side effects.¹⁰⁻¹³

Recently, we reported that carbazole derivative **1** with the 2-CF₃ group showed potent KSP inhibitory activity (Figure 1).¹⁴ Carbazole derivatives, with a lactam ring (**2**) or urea group (**4c**), and the β -carboline derivative **3a** were also identified as highly potent KSP inhibitors by structure–activity relationship studies of **1**.¹⁵ However, these inhibitors exhibited limited solubility in the aqueous solvents employed for in vivo studies. To satisfy the potent inhibitory activity requirements as well as better solubility in aqueous solution, we have designed diphenylamine derivatives such as **5a** by modification of the planar carbazole-type inhibitor **2**.¹⁶ Diphenylamine **5a** exhibited better solubility than carbazole **2** while maintaining potent KSP inhibitory activity. Structural analysis by single crystal X-ray diffraction studies and free energy calculations demonstrated that the improved solubility of **5a** is attributed to fewer van der Waals interactions in the crystal packing, as well as a hydrogen-bond acceptor nitrogen in the aniline moiety for favorable solvation. Interestingly, compound **5a** possibly binds to the interface of the α 4 and α 6 of KSP in an ATP-competitive manner, whereas most KSP inhibitors (e.g., monastrol, *S*-trityl-L-cysteine) bind to the allosteric pocket formed by helices α 2, α 3 and loop L5 to show ATP-uncompetitive behavior.¹⁷⁻¹⁹ Replacing the right-hand 3-CF₃-phenyl group in **5a** with a pyridine ring provided a more soluble KSP inhibitor **6**; however, this compound showed slightly lower potency than **5a**.¹⁶ In this article, we describe the structure–activity relationship study for novel diaryl amine-type KSP inhibitors with high potency and aqueous solubility. For this purpose, we performed: (i) modification of ring-fused indoles such as **3a** and **4c** using the same approach employed for the development of **5a** and (ii) intensive optimization studies of diphenylamine **5a**.

2. Results and discussion

2.1. Investigation of diaryl amine-type KSP inhibitors by modification of ring-fused

scaffolds

We speculated that the poor solubility of carboline and carbazole derivatives would be attributable to the significant intermolecular interactions in the crystals (e.g., π - π stacking interactions) as seen for compound **2**.¹⁶ To disrupt the possible crystal packing of compounds **3a** and **4c**, the design of less planar analogs was expected to be a promising approach.²⁰ Therefore, we designed diaryl amine derivatives **7** and **8**, in which the pyrrole C-C bond in the central part of carbolines **3** and carbazoles **4** was cleaved (Figure 2). Diaryl amines **7a,b** with a pyridine ring were designed based on carbolines **3a,b** with potent KSP inhibitory activity (Figure 2A). Diphenylamines **8a-f** with a nitro, amino or urea group at the 3- or 4-position on the left-hand phenyl ring were similarly investigated, which represent the cleaved analogs of carbazoles **4b-f** (Figure 2B). Diaryl amine derivatives **7a,b** and **8a,d** were prepared by palladium-catalyzed *N*-arylation using aryl bromides **9** and substituted anilines **10** (Scheme 1).²¹ For the preparation of compounds **8c,f** with a urea group, nitro derivatives **8a,d** were reduced to the corresponding amines **8b,e** using Pd/C and ammonium formate, which were converted to the expected compounds **8c,f** by KOCN.

First, KSP inhibitory activity of compounds **7a,b**, with a pyridine ring in the left-hand part, was comparatively assessed with the parent carboline-type inhibitors **3a,b** (Table 1). Unfortunately, the cleavage of the pyrrole C-C bond in carboline led to loss of KSP ATPase inhibitory activity at 6.3 μ M. The solubility of these compounds was evaluated by a thermodynamic method.²² A mixture of EtOH-phosphate buffer (pH 7.4) (1:1) [50% EtOH] and phosphate buffer (pH 7.4) were employed as aqueous media.²² In these solutions, the parent carbazole-type inhibitor **1** was moderately soluble (0.424 mg/mL) and insoluble (<1 μ g/mL), respectively. *N*-(Pyridin-3-yl)amine **7a** showed the anticipated improvement in thermodynamic solubility, being 30 times more soluble in 50% EtOH (14.3 mg/mL) compared with the corresponding carboline **3a**. *N*-(Pyridin-4-yl)amine **7b** also exhibited

approximately 14 times greater solubility in 50% EtOH (24.0 mg/mL) than the parent carboline **3b**. Of note, compound **7b** had moderate solubility (264 µg/mL) even in phosphate buffer, which was 80 times or more soluble compared with **3b** and **3a**, respectively. Although these pyridinylamine derivatives **7a,b** were inert in KSP inhibition, it was suggested that cleavage of the pyrrole C–C bond in carboline and carbazole derivatives could be a promising approach to improve the solubility in aqueous solution.

Diphenylamine derivatives **8a–f** with a nitro, amino or urea group at the 3- or 4-position on the left-hand phenyl group were next examined (Table 2). The 3-substituted anilines **8a–c** showed no KSP inhibitory activity at 6.3 µM. Among the 4-substituted analogs, compound **8f** with a urea group exhibited moderate inhibitory activity ($IC_{50} = 0.39 \mu\text{M}$), while compounds **8d,e** with a nitro or amino group had weak or no potency. The potency of **8f** was approximately three times lower than that of the parent carbazole **4f**.

2.2. Optimization studies of lactam-fused diaryl amine-type KSP inhibitors

Next, we investigated the structure–activity relationship and the further refinement of **5a** for novel potent KSP inhibitors in terms of: (i) the linkage between the two aryl groups, (ii) the substituent on the right-hand phenyl group, (iii) the left-hand heterocycle, and (iv) the right-hand aromatic heterocycle (Figure 3).

A series of diaryl amine derivatives **5** and **11–14** were prepared by Buchwald–Hartwig *N*-arylation using aryl bromides or triflates **9** and substituted anilines **10**, except for the compounds (**11j,l,n** and **12c,k**) indicated below (Scheme 1).²¹ Diphenylether derivative **17a** was obtained by treatment of phenol derivative **15** with diaryliodonium tetrafluoroborate **16** in the presence of $KOt\text{-Bu}$.²³ Diphenylsulfide derivatives **20a,b** were prepared by the copper-catalyzed C–S bond-forming reaction using aryl thiol **18** and CF_3 -substituted iodobenzenes **19a,b**.²⁴ Compounds **11j**, **11l**, **11n** and **12k** were obtained by simple

transformations including BBr₃-mediated demethylation of **11h**, Zn-mediated reduction of **11k**, saponification of **11m**, and thiocarbonylation of **5a** using Lawesson's reagent,²⁵ respectively. Compound **12c** was prepared by treatment of **12a** with O₂ in the presence of Pd(OAc)₂.

We initially investigated the type of heteroatom in the central part of diphenylamine **5a** and the position of a substituent on the right-hand phenyl group (Table 3). Replacing the bridging NH group in compound **5a** with oxygen (**17a,b**: ether) or sulfur (**20a,b**: thioether) resulted in a significant reduction or loss of KSP inhibitory activity. This indicates that the aniline NH group of **5a** is an indispensable functional group as a hydrogen-bond donor, which is supported by our previous modeling study.¹⁶ Regarding the position of CF₃ group on the right-hand phenyl ring of **5a**, 4-CF₃ compound **5b** was approximately 7 times less potent than **5a** and no KSP inhibition of 2-CF₃ compound **5c** was observed.

Next, the structure–activity relationship was examined by replacing 3-substituents on the right-hand phenyl group in **5a** (Table 4). Among compounds **11a–d** with or without a 3-alkyl substituent, the *tert*-butyl derivative **11d** exhibited the most potent inhibitory activity (IC₅₀ = 0.16 μM). The structure–activity relationship of the simple alkyl group correlated with that of the carbazole-type KSP inhibitors, suggesting that carbazoles (**1** and **2**) and diphenylamines (**5a** and **11d**) may occupy the same binding site of KSP.^{15,16} Substitution with 3,5-di-CF₃ (**11e**), 3-phenyl (**11f**), 3-phenoxy (**11g**) and 3-methoxy (**11h**) groups were not effective. Introduction of a polar substituent such as 3-hydroxy (**11j**), 3-amino (**11i**), 3-methoxycarbonyl (**11m**), or 3-carboxylate (**11n**) also gave rise to inactive compounds. 3-Trifluoromethoxy (**11i**) and 3-nitro (**11k**) derivatives showed moderate inhibitory activity. It is inferred from these data that the substituent at the 3-position on the right-hand phenyl part is buried in a relatively large hydrophobic pocket of KSP. The possible binding mode of **11d** to the interface of the α4 and α6 helices of KSP is shown in Figure 5. The *tert*-butyl group of **11d** was buried in the

deep hydrophobic pocket formed by Tyr104, Gly296, Ile299, Thr300, Ile332, Tyr352, Ala353, and Ala356. Low desolvation energy of *tert*-butyl group compared with smaller alkyl groups may also contribute to the favorable binding of **11d** to KSP.

In the left part of the molecule, the position of accessory amide group was crucial for the potency (Table 5). Compounds **12a–d** with an amide group at the 3-position were less active or inactive, while the parent compound **5a** with the 4-position amide group showed potent KSP inhibitory activity. A five-membered ring thiocarbamate **12g** exhibited moderate inhibitory activity ($IC_{50} = 0.81 \mu M$) in contrast to the ineffectiveness in lactam derivative **12e** and carbamate derivative **12f**, suggesting that the introduction of a sulfur atom into the lactam ring had favorable effects on the bioactivity. The addition of a sulfur atom (**12i**) into the six-membered lactam of **5a** also maintained potent KSP inhibitory activity ($IC_{50} = 0.051 \mu M$), whereas an oxygen atom (**12h**) decreased the inhibitory activity. The loss of activity in the *N*-methylamide derivative **12j** indicates that the lactam NH group at this position is essential for KSP inhibition. Compound **12k**, with a thioamide group, had slightly reduced potency ($IC_{50} = 0.19 \mu M$) compared with **5a**. Compound **12l**, with a seven-membered lactam, showed approximately equipotent KSP inhibitory activity ($IC_{50} = 0.050 \mu M$) to **5a**, suggesting that some flexibility of the lactam carbonyl placement is tolerated. Substitution with a fluorine group on the 5- or 6-position (**12m,n**) resulted in a reduction in the inhibitory activity, suggesting that modification at these positions was inappropriate for favorable interactions with KSP.

2.3. Analysis of aqueous solubility of potent KSP inhibitors and further optimization

The thermodynamic solubility of potent diphenylamine derivatives **12i,l** in aqueous media was next evaluated (Table 6).²² Diphenylamine **12i** with a thiomorpholin-3-one structure was slightly less soluble (1.70 mg/mL in 50% EtOH) than the parent compound **5a**. The longer

retention time on a reversed-phase HPLC column (28.2 min) of compound **12i** indicated that the introduction of a sulfur atom into the lactam ring of **5a** resulted in the increased hydrophobicity, thereby lowering the solubility in aqueous media. Diphenylamine **12i** with a seven-membered lactam ring was approximately four times more soluble (7.39 mg/mL in 50% EtOH) than **5a**, although a high CLogP value and HPLC retention time indicated higher hydrophobicity. The lower melting point of compound **12i** (140 °C) suggested that the weak crystal packing mainly contributed to the observed improvement in solubility. These results indicated that the seven-membered lactam ring on the left-hand phenyl group was a promising structural unit for the development of KSP inhibitors that have a favorable balance of bioactivity and aqueous solubility.

As such, we identified benzothiomorpholin-3-one **12i** and benzoazepin-2-one **12i** as potent KSP inhibitors using structure–activity relationship studies of fused heterocycles on the left-hand phenyl group. Compound **12i** represents the lead compound for further structural refinements because of the improved solubility. Separately, examination of the right-hand phenyl group identified 6-pyridine derivative **6** with potent KSP inhibitory activity and improved aqueous solubility.¹⁶ On the basis of these promising components, two diaryl amine derivatives were then designed (Figure 4). Diaryl amine **13** was designed based on compound **12i** with a thiomorpholin-3-one structure and compound **6** with a 6-pyridine ring. Diaryl amine **14** was similarly designed based on compounds **12i** and **6**.

Thiomorpholin-3-one **13** exhibited the most potent KSP inhibitory activity ($IC_{50} = 0.035$ μ M) among the diaryl amine-type inhibitors that were examined in this study (Table 6). However, compound **13** was less soluble in 50% EtOH (0.669 mg/mL) and in phosphate buffer (1.11 μ g/mL) than the parent compound **6**. The high melting point of compound **13** (217 °C) indicated that the tight crystal packing might cause this decrease in aqueous solubility. Benzoazepin-2-one **14** maintained highly potent KSP inhibitory activity ($IC_{50} =$

0.050 μM) as seen for the parent compounds **5a**, **6** and **12l**. Compound **14** exhibited greater solubility in 50% EtOH (4.82 mg/mL) and in phosphate buffer (8.07 $\mu\text{g/mL}$) than the corresponding compound **6**. Of note, solubility of compound **14** in phosphate buffer was remarkably improved, as we expected, in comparison with compound **12l** (less than 1 $\mu\text{g/mL}$), although **14** was less soluble than **12l** in 50% EtOH. Taken together, compound **14** was identified to be a novel KSP inhibitor with a favorable balance of potency and aqueous solubility.

Compounds **5a**, **6**, **12i,l**, **13** and **14** were tested for their inhibitory effect on the proliferation of cancer cell lines: lung cancer cells A549, colorectal cancer cells HCT-116, and breast cancer cells MCF-7 (Table 7). Cells were treated with increasing concentrations of the compounds, and viabilities were measured by the 3-(4,5-dimethylthiazol-2-yl)-5-(3-carboxymethoxyphenyl)-2-(4-sulfophenyl)-2*H*-tetrazolium (MTS) assay. All the tested diaryl amine derivatives were shown to be effective against these cell lines. In particular, thiomorpholin-3-one derivative **13** with the highest KSP inhibitory activity was found to be the most potent against all the cell lines tested.²⁶

3. Conclusions

We have performed structure–activity relationship studies for the development of novel KSP inhibitors using carbolines **3**, carbazoles **4** and diphenylamine **5a** as the lead compounds. Unfortunately, the nonplanar analogs **7** and **8** of planar carbolines **3** and carbazoles **4** decreased the potency for KSP inhibition. Optimization studies of diphenylamine **5a** revealed that bridging NH group, 3- CF_3 group on the right-hand phenyl group, and the lactam amide group at the 4-position on the left-hand phenyl group contributed to the potent KSP inhibitory activity. Further investigations provided novel KSP inhibitors **13** with the most potent inhibitory activity and **14** with the optimal balance of potency and aqueous solubility in this

study.

4. Experimental

4.1. Synthesis

4.1.1. General methods

¹H NMR spectra were recorded using a JEOL AL-400 or a JEOL ECA-500 spectrometer. Chemical shifts are reported in δ (ppm) relative to Me₄Si as an internal standard. ¹³C NMR spectra were referenced to the residual DMSO signal. Exact mass (HRMS) spectra were recorded on a JMS-HX/HX 110A mass spectrometer. Melting points were measured by a hot stage melting point apparatus (uncorrected). For flash chromatography, Wakogel C-300E (Wako) or Chromatorex[®] NH was employed. For analytical HPLC, a Cosmosil 5C18-ARII column (4.6 x 250 mm, Nacalai Tesque, Inc., Kyoto, Japan) was employed with a linear gradient of CH₃CN containing 0.1% (v/v) TFA at a flow rate of 1 mL/min on a Shimadzu LC-10ADvp (Shimadzu Corp., Ltd., Kyoto, Japan), and eluting products were detected by UV at 254 nm. The purity of the compounds was determined by combustion analysis or HPLC analysis (> 95%).

4.1.2. General procedure of *N*-arylation for preparation of diaryl amine compounds: synthesis of 6-{{3-(trifluoromethoxy)phenyl}amino}-3,4-dihydroquinolin-2(1*H*)-one (11i)

Toluene (4.5 mL) was added to a flask containing 6-bromo-3,4-dihydroquinolin-2(1*H*)-one (300 mg, 1.33 mmol), 3-(trifluoromethoxy)aniline (231 μ L, 1.73 mmol), Pd₂(dba)₃ (15.2 mg, 0.02 mmol), 2-dicyclohexylphosphino-2',4',6'-triisopropylbiphenyl (31.6 mg, 0.07 mmol) and NaOt-Bu (192 mg, 2.00 mmol) under an argon atmosphere. The mixture was stirred at 100 °C for 9 h. After cooling, the reaction mixture was diluted with EtOAc, and filtered through a pad of Celite. The filtrate was concentrated *in vacuo*. Crude material was purified by flash

chromatography with *n*-hexane/EtOAc (2:3) to afford the desired diaryl amine **11i** (292 mg, 68% yield): pale yellow solid; mp 160-162 °C; IR (neat) cm^{-1} : 1667 (C=O), 3219 (NH), 3315 (NH); ^1H NMR (500 MHz, DMSO- d_6) δ 2.43 (t, $J = 6.9$ Hz, 2H; CH₂), 2.85 (t, $J = 6.9$ Hz, 2H; CH₂), 6.63 (d, $J = 8.0$ Hz, 1H; Ar), 6.79 (s, 1H; Ar), 6.81 (d, $J = 8.0$ Hz, 1H; Ar), 6.91-6.96 (m, 3H; Ar), 7.25 (t, $J = 8.0$ Hz, 1H; Ar), 8.25 (s, 1H; NH), 9.99 (s, 1H; NH); ^{13}C NMR (125 MHz, DMSO- d_6) δ 25.0, 30.4, 106.3, 109.6, 113.1, 115.8, 118.7, 119.5, 120.1 (q), 124.7, 130.7, 133.1, 136.1, 146.9, 149.4, 169.8; *Anal.* calcd for C₁₆H₁₃F₃N₂O₂: C, 59.63; H, 4.07; N, 8.69. Found: C, 59.51; H, 4.12; N, 8.59.

4.1.3. *N*¹-[3-(Trifluoromethyl)phenyl]benzene-1,3-diamine (**8b**)

To a stirred solution of 3-nitro-*N*-[3-(trifluoromethyl)phenyl]aniline **8a** (190 mg, 0.67 mmol) and ammonium formate (509 mg, 8.07 mmol) in EtOH (2.2 mL) at room temperature was added 10% Pd/C (35.8 mg, 0.03 mmol). The mixture was heated under reflux for 2 h. After cooling, the reaction mixture was diluted with EtOAc, and filtered through a pad of Celite. The filtrate was concentrated *in vacuo*. Crude material was purified by flash chromatography with *n*-hexane/EtOAc (3:1) to afford compound **8b** (165 mg, 97%): brown oil; IR (neat) cm^{-1} : 3035 (NH), 3377 (NH); ^1H NMR (400 MHz, DMSO- d_6) δ 4.96 (s, 2H; NH₂), 6.19 (d, $J = 8.0$ Hz, 1H; Ar), 6.28 (d, $J = 8.0$ Hz, 1H; Ar), 6.37 (s, 1H; Ar), 6.92 (t, $J = 8.0$ Hz, 1H; Ar), 7.01 (d, $J = 8.0$ Hz, 1H; Ar), 7.22 (s, 1H; Ar), 7.25 (d, $J = 8.2$ Hz, 1H; Ar), 7.37 (t, $J = 8.0$ Hz, 1H; Ar), 8.13 (s, 1H; NH); ^{13}C NMR (125 MHz, DMSO- d_6) δ 104.0, 106.5, 107.8, 111.3, 114.3, 118.8, 124.3 (q), 129.6, 129.8 (q), 130.0, 142.5, 145.2, 149.7; HRMS (FAB): *m/z* calcd for C₁₃H₁₁F₃N₂ (M⁺) 252.0874; found: 252.0874.

4.1.4. 1-(3-{[3-(Trifluoromethyl)phenyl]amino}phenyl)urea (**8c**)

To a stirred solution of *N*¹-[3-(trifluoromethyl)phenyl]benzene-1,3-diamine **8b** (80.0 mg,

0.32 mmol) in AcOH (4.0 mL) was added KOCN (77.2 mg, 0.95 mmol) and water (80.0 μ L). The reaction mixture was stirred at room temperature for 18 h, then evaporated to dryness under vacuum. Crude material was purified by flash chromatography with amino silica gel with CHCl₃/MeOH (20:1 to 10:1) to afford compound **8c** (31.9 mg, 34% yield): yellow oil; IR (neat) cm⁻¹: 1661 (C=O), 3225 (NH), 3351 (NH); ¹H NMR (500 MHz, DMSO-*d*₆) δ 5.82 (br, 2H; NH₂), 6.66 (d, *J* = 8.0 Hz, 1H; Ar), 6.84 (d, *J* = 8.0 Hz, 1H; Ar), 7.06 (d, *J* = 8.0 Hz, 1H; Ar), 7.12 (t, *J* = 8.0 Hz, 1H; Ar), 7.28 (s, 1H; Ar), 7.30 (d, *J* = 8.0 Hz, 1H; Ar), 7.41 (s, 1H; Ar), 7.42 (t, *J* = 8.0 Hz, 1H; Ar), 8.50 (br, 2H; NH); ¹³C NMR (125 MHz, DMSO-*d*₆) δ 107.4, 110.7, 110.9, 111.5, 114.8, 118.9, 124.2 (q), 129.3, 129.8 (q), 130.1, 141.5, 142.2, 144.6, 155.8; HRMS (FAB): *m/z* calcd for C₁₄H₁₂F₃N₃O (M⁺) 295.0932; found: 295.0926.

4.1.5. 6-[(3-Hydroxyphenyl)amino]-3,4-dihydroquinolin-2(1*H*)-one (**11j**)

A suspension of 6-[(3-methoxyphenyl)amino]-3,4-dihydroquinolin-2(1*H*)-one **11h** (500 mg, 1.86 mmol) in dry CH₂Cl₂ (5 mL) was cooled to -78 °C and then BBr₃ (7.45 mL of 1 M solution in CH₂Cl₂, 7.45 mmol) was added. After the mixture was stirred for 30 min at -78 °C, the stirring was continued for additional 18 h at room temperature. The reaction was quenched by addition of water (12 mL), and CH₂Cl₂ was removed under reduced pressure. The aqueous solution was neutralized by addition of aqueous NaOH, and then extracted three times with EtOAc. The organic layer was washed with brine, and dried over Na₂SO₄. The organic solvent was removed under reduced pressure and the crude residue was purified by flash chromatography with *n*-hexane/EtOAc (1:3) to afford compound **11j** (232 mg, 49% yield): brown needle crystal; mp 213-214 °C; IR (neat) cm⁻¹: 1651 (C=O), 3222 (NH), 3321 (NH); ¹H NMR (500 MHz, DMSO-*d*₆) δ 2.41 (t, *J* = 7.4 Hz, 2H; CH₂), 2.81 (t, *J* = 7.4 Hz, 2H; CH₂), 6.15 (d, *J* = 8.0 Hz, 1H; Ar), 6.38 (d, *J* = 8.0 Hz, 1H; Ar), 6.39 (s, 1H; Ar), 6.74 (d, *J* = 8.0 Hz, 1H; Ar), 6.85 (d, *J* = 8.0 Hz, 1H; Ar), 6.89 (s, 1H; Ar), 6.94 (t, *J* = 8.0 Hz, 1H; Ar), 7.77 (s,

1H; NH), 9.07 (s, 1H; OH), 9.89 (s, 1H; NH); ¹³C NMR (125 MHz, DMSO-*d*₆) δ 25.1, 30.5, 102.2, 106.0, 106.6, 115.6, 117.4, 118.2, 124.4, 129.7, 131.7, 137.7, 145.8, 158.1, 169.7; *Anal.* calcd for C₁₅H₁₄N₂O₂: C, 70.85; H, 5.55; N, 11.02. Found: C, 71.11; H, 5.59; N, 10.89.

4.1.6. 6-[(3-Aminophenyl)amino]-3,4-dihydroquinolin-2(1H)-one (11l)

To a stirred solution of 6-[(3-nitrophenyl)amino]-3,4-dihydroquinolin-2(1H)-one **11k** (62.0 mg, 0.22 mmol) in AcOH (2.2 mL) at room temperature was added zinc powder (102 mg, 1.56 mmol) portionwise. After being stirred at room temperature for 1 h, the reaction mixture was filtered through a pad of Celite and concentrated under vacuum. The residue was diluted with EtOAc, and the whole was washed with saturated NaHCO₃, brine, and dried over Na₂SO₄. The organic solvent was removed under reduced pressure and the crude residue was purified by flash chromatography with *n*-hexane/EtOAc (1:8) to afford compound **11l** (41.6 mg, 75% yield): pale yellow solid; mp 196-198 °C; IR (neat) cm⁻¹: 1662 (C=O), 3221 (NH), 3344 (NH); ¹H NMR (500 MHz, DMSO-*d*₆) δ 2.40 (t, *J* = 7.4 Hz, 2H; CH₂), 2.80 (t, *J* = 7.4 Hz, 2H; CH₂), 4.93 (br, 2H; NH₂), 6.00 (d, *J* = 8.0 Hz, 1H; Ar), 6.15 (d, *J* = 8.0 Hz, 1H; Ar), 6.24 (s, 1H; Ar), 6.72 (d, *J* = 8.0 Hz, 1H; Ar), 6.80 (d, *J* = 8.0 Hz, 1H; Ar), 6.83 (d, *J* = 8.0 Hz, 1H; Ar), 6.86 (s, 1H; Ar), 7.58 (s, 1H; NH), 9.87 (s, 1H; NH); ¹³C NMR (125 MHz, DMSO-*d*₆) δ 25.2, 30.5, 101.4, 104.5, 105.7, 115.5, 116.9, 117.7, 124.3, 129.3, 131.2, 138.3, 145.0, 149.2, 169.6; HRMS (FAB): calcd for C₁₅H₁₅N₃O (M⁺) 253.1215; found: 253.1213.

4.1.7. 3-[(2-Oxo-1,2,3,4-tetrahydroquinolin-6-yl)amino]benzoic acid (11n)

To a solution of methyl 3-[(2-oxo-1,2,3,4-tetrahydroquinolin-6-yl)amino]benzoate **11m** (400 mg, 1.35 mmol) in 5.2 mL of MeOH/H₂O (3:1 v/v) was added LiOH·H₂O (170 mg, 4.05 mmol) at 0 °C, then the solution was warmed to 50 °C. After 1 h, the reaction mixture was acidified to below pH 2 using 1 M HCl, then EtOAc and brine were added to the mixture. The

organic extracts were washed with brine and dried over Na₂SO₄. The organic solvent was removed under reduced pressure to afford compound **11n** (366 mg, 96% yield): white solid; mp 259-261 °C; IR (neat) cm⁻¹: 1656 (C=O), 1684 (C=O), 3203 (NH), 3326 (NH); ¹H NMR (500 MHz, DMSO-*d*₆) δ 2.43 (t, *J* = 7.4 Hz, 2H; CH₂), 2.85 (t, *J* = 7.4 Hz, 2H; CH₂), 6.81 (d, *J* = 8.0 Hz, 1H; Ar), 6.93 (d, *J* = 8.0 Hz, 1H; Ar), 6.94 (s, 1H; Ar), 7.17 (d, *J* = 8.0 Hz, 1H; Ar), 7.27-7.31 (m, 2H; Ar), 7.53 (s, 1H; Ar), 8.12 (s, 1H; NH), 9.98 (s, 1H; NH), 12.78 (br, 1H; CO₂H); ¹³C NMR (125 MHz, DMSO-*d*₆) δ 25.1, 30.4, 115.5, 115.8, 118.1, 118.9, 119.0, 119.2, 124.6, 129.3, 131.7, 132.6, 136.9, 145.2, 167.6, 169.8; HRMS (FAB): *m/z* calcd for C₁₆H₁₄N₂O₃ (M⁺) 282.1004; found: 282.1011.

4.1.8. 7-{[3-(Trifluoromethyl)phenyl]amino}quinolin-2(1*H*)-one (**12c**)

AcOH (1.0 mL) was added to a flask containing 7-{[3-(trifluoromethyl)phenyl]amino}-3,4-dihydroquinolin-2(1*H*)-one **12a** (80.0 mg, 0.26 mmol) and Pd(OAc)₂ (22.4 mg, 0.10 mmol) and an oxygen balloon was connected to the reaction vessel. After stirring for 2 h at 115 °C, the reaction mixture was cooled to room temperature and concentrated *in vacuo*. The residue was purified by flash chromatography with *n*-hexane/EtOAc (1:3 to 1:5) to afford **12c** (34.1 mg, 43% yield): white solid; mp 177–179 °C; IR (neat) cm⁻¹: 1655 (C=O), 3452 (NH); ¹H NMR (500 MHz, DMSO-*d*₆) δ 6.24 (d, *J* = 9.2 Hz, 1H; C=CH), 6.88 (dd, *J* = 8.0, 2.3 Hz, 1H; Ar), 7.06 (d, *J* = 2.3 Hz, 1H; Ar), 7.23 (d, *J* = 8.0 Hz, 1H; Ar), 7.41 (s, 1H; Ar), 7.45 (d, *J* = 8.0 Hz, 1H; Ar), 7.50–7.53 (m, 2H; Ar), 7.75 (d, *J* = 9.2 Hz, 1H; C=CH), 8.99 (s, 1H; NH), 11.53 (s, 1H; NH); ¹³C NMR (125 MHz, DMSO-*d*₆) δ 99.7, 112.3, 113.1, 113.5, 116.7, 117.7, 121.0, 124.1 (q), 129.0, 130.0 (q), 130.4, 139.8, 140.5, 142.9, 144.5, 162.2; HRMS (FAB): *m/z* calcd for C₁₆H₁₁F₃N₂O [M + H]⁺ 305.0902; found: 305.0905.

4.1.9. 6-{[3-(Trifluoromethyl)phenyl]amino}-3,4-dihydroquinoline-2(1H)-thione (12k)

To a stirred solution of 6-{[3-(trifluoromethyl)phenyl]amino}-3,4-dihydroquinolin-2(1H)-one **5a** (50.0 mg, 0.16 mmol) in toluene (1.0 mL) was added Lawesson's reagent (33.0 mg, 0.08 mmol) under an argon atmosphere. After stirring for 30 min at 110 °C, the reaction mixture was cooled to room temperature and concentrated *in vacuo*. The residue was purified by flash chromatography with *n*-hexane/EtOAc (3:1) to afford **12k** (51.4 mg, 100% yield): yellow solid; mp 195–196 °C; IR (neat) cm^{-1} : 1499 (C=S), 3361 (NH); ^1H NMR (500 MHz, DMSO- d_6) δ 2.77 (t, $J = 8.0$ Hz, 2H; CH₂), 2.90 (t, $J = 8.0$ Hz, 2H; CH₂), 6.97 (s, 1H; Ar), 6.98 (d, $J = 8.0$ Hz, 1H; Ar), 7.04 (d, $J = 8.0$ Hz, 1H; Ar), 7.06 (d, $J = 8.0$ Hz, 1H; Ar), 7.20 (s, 1H; Ar), 7.27 (d, $J = 8.0$ Hz, 1H; Ar), 7.41 (d, $J = 8.0$ Hz, 1H; Ar), 8.49 (s, 1H; NH), 12.15 (s, 1H; NH); ^{13}C NMR (125 MHz, DMSO- d_6) δ 24.0, 38.9, 111.4, 114.9, 117.0, 117.3, 118.3, 118.5, 124.3 (q), 126.6, 130.0 (q), 130.3, 131.3, 138.3, 144.9, 197.3; HRMS (FAB): m/z calcd for C₁₆H₁₃F₃N₂S (M⁺) 322.0752; found: 322.0758.

4.1.10. 7-{[4-(Trifluoromethyl)pyridin-2-yl]amino}-2H-benzo[*b*][1,4]thiazin-3(4H)-one (13)

Following the general procedure for **11i**, compound **13** (48.5 mg, 12% yield) was synthesized from 7-bromo-2H-benzo[*b*][1,4]thiazin-3(4H)-one and 2-amino-4-(trifluoromethyl)pyridine: white solid; mp 217–218 °C; IR (neat) cm^{-1} : 1688 (C=O), 3194 (NH); ^1H NMR (500 MHz, DMSO- d_6) δ 3.45 (s, 2H; CH₂), 6.92 (d, $J = 8.6$ Hz, 1H; Ar), 6.99 (d, $J = 5.2$ Hz, 1H; Ar), 7.03 (s, 1H; Ar), 7.33 (dd, $J = 8.6, 1.7$ Hz, 1H; Ar), 7.81 (d, $J = 1.7$ Hz, 1H; Ar), 8.37 (d, $J = 5.2$ Hz, 1H; Ar), 9.43 (s, 1H; NH), 10.44 (s, 1H; NH); ^{13}C NMR (125 MHz, DMSO- d_6) δ 29.1, 106.2, 108.6, 117.1, 117.5, 117.7, 119.3, 123.0 (q), 131.7, 135.9, 137.6 (q), 149.3, 156.1, 164.8; HRMS (FAB): m/z calcd for C₁₄H₁₀F₃N₃OS (M⁺) 325.0497; found: 325.0497.

4.1.11. 7-[4-(Trifluoromethyl)pyridin-2-yl]amino}-1,3,4,5-tetrahydro-2H-benzo[b]azepin-2-one (14)

Following the general procedure for **11i**, compound **14** (16.7 mg, 18% yield) was synthesized from 7-bromo-1,3,4,5-tetrahydro-2H-benzo[b]azepin-2-one and 2-amino-4-(trifluoromethyl)pyridine: pale yellow solid; mp 185–187 °C; IR (neat) cm^{-1} : 1688 (C=O), 2936 (NH); ^1H NMR (500 MHz, DMSO- d_6) δ 2.09–2.16 (m, 4H; CH₂ × 2), 2.67 (t, J = 6.9 Hz, 2H; CH₂), 6.92 (d, J = 8.0 Hz, 1H; Ar), 6.98 (d, J = 5.2 Hz, 1H; Ar), 7.07 (s, 1H; Ar), 7.53 (d, J = 8.0 Hz, 1H; Ar), 7.55 (s, 1H; Ar), 8.37 (d, J = 5.2 Hz, 1H; Ar), 9.36 (s, 1H; NH), 9.42 (s, 1H; NH); ^{13}C NMR (125 MHz, DMSO- d_6) δ 27.8, 30.1, 32.7, 106.0, 108.4, 117.4, 119.6, 121.9, 122.0, 123.0 (q), 132.7, 134.1, 137.4, 137.5 (q), 149.3, 156.3, 173.1; HRMS (FAB): m/z calcd for C₁₆H₁₄F₃N₃O (M⁺) 321.1089; found: 321.1092.

4.1.12. 6-[3-(Trifluoromethyl)phenoxy]-3,4-dihydroquinolin-2(1H)-one (17a)

To a suspension of KO t -Bu (60.5 mg, 0.54 mmol) in DMF (2.1 mL) was added 6-hydroxy-3,4-dihydroquinolin-2(1H)-one **15** (80.0 mg, 0.49 mmol) at 0 °C and the reaction mixture was stirred at this temperature for 15 min. Bis(3-trifluoromethylphenyl)iodonium tetrafluoroborate **16** (259 mg, 0.51 mmol) was added in one portion and the reaction mixture was stirred at 40 °C for 1 h, then quenched with H₂O at 0 °C and extracted into CHCl₃. The organic layer was washed with brine, and dried over Na₂SO₄. The organic solvent was removed under reduced pressure and the crude residue was purified by flash chromatography with *n*-hexane/EtOAc (1:1) to afford compound **17a** (39.9 mg, 27% yield): white solid; mp 158–159 °C; IR (neat) cm^{-1} : 1681 (C=O), 3203 (NH); ^1H NMR (500 MHz, DMSO- d_6) δ 2.44 (t, J = 7.4 Hz, 2H; CH₂), 2.87 (t, J = 7.4 Hz, 2H; CH₂), 6.91 (s, 2H; Ar), 6.99 (s, 1H; Ar), 7.20–7.23 (m, 2H; Ar), 7.42 (d, J = 8.0 Hz, 1H; Ar), 7.58 (t, J = 8.0 Hz, 1H; Ar), 10.12 (s, 1H;

NH); ^{13}C NMR (125 MHz, DMSO- d_6) δ 24.7, 30.0, 113.6, 116.3, 118.7, 119.1, 119.5, 121.0, 123.7 (q), 125.7, 130.6 (q), 131.2, 135.3, 149.6, 158.4, 169.9; HRMS (FAB): m/z calcd for $\text{C}_{16}\text{H}_{12}\text{F}_3\text{NO}_2$ (M^+) 307.0820; found: 307.0826.

4.1.13. 6- $\{[3\text{-(Trifluoromethyl)phenyl}]\text{thio}\}$ -3,4-dihydroquinolin-2(1H)-one (**20a**)

2-Propanol (1.0 mL) was added to a flask containing 6-mercapto-3,4-dihydroquinolin-2(1H)-one **18** (50.0 mg, 0.28 mmol), 3-trifluoromethyliodobenzene **19a** (40.4 μL , 0.28 mmol), CuI (32.0 mg, 0.17 mmol), ethylene glycol (31.2 μL , 0.56 mmol) and K_2CO_3 (96.7 mg, 0.70 mmol) under an argon atmosphere. The mixture was stirred at 80 $^\circ\text{C}$ for 13 h. After cooling, the reaction mixture was diluted with EtOAc, and filtered through a pad of Celite. The filtrate was concentrated *in vacuo*. Crude material was purified by flash chromatography with *n*-hexane/EtOAc (3:2) to afford compound **20a** (6.2 mg, 7% yield): white solid; mp 102-104 $^\circ\text{C}$; IR (neat) cm^{-1} : 1676 (C=O), 3387 (NH); ^1H NMR (500 MHz, DMSO- d_6) δ 2.53 (t, $J = 7.4$ Hz, 2H; CH_2), 2.96 (t, $J = 7.4$ Hz, 2H; CH_2), 7.00 (d, $J = 8.0$ Hz, 1H; Ar), 7.40 (d, $J = 8.0$ Hz, 1H; Ar), 7.42-7.45 (m, 2H; Ar), 7.49 (s, 1H; Ar), 7.58-7.59 (m, 2H; Ar), 10.34 (s, 1H; NH); ^{13}C NMR (125 MHz, DMSO- d_6) δ 24.4, 30.0, 116.4, 122.4, 122.6, 123.0, 123.7 (q), 125.4, 129.9 (q), 130.3, 131.0, 133.5, 133.7, 139.5, 140.1, 170.1; HRMS (FAB): m/z calcd for $\text{C}_{16}\text{H}_{12}\text{F}_3\text{NOS}$ (M^+) 323.0592; found: 323.0591.

4.2. KSP ATPase assay

The microtubules-stimulated KSP ATPase reaction was performed in a reaction buffer [20 mM PIPES-KOH (pH 6.8), 25 mM KCl, 2 mM MgCl_2 , 1 mM EGTA-KOH (pH 8.0)] containing 38 nM of the bacteria-expressed KSP motor domain (1–369) fused to histidine-tag at the carboxyl-terminus and 350 nM microtubules in 96-well half-area plates (Corning). Each

chemical compound in DMSO at different concentrations was diluted 12.5-fold with the chemical dilution buffer [10 mM Tris-OAc (pH7.4), 0.04% (v/v) NP-40]. After pre-incubation of 9.7 μ L of the enzyme solution with 3.8 μ L of each chemical solution at 25 °C for 30 min, the ATPase reaction was initiated by the addition of 1.5 μ L of 0.3 mM ATP solution, and followed by incubation at 25 °C for further 15 min. The reaction was terminated by the addition of 15 μ L of the Kinase-Glo Plus reagent (Promega). The ATP consumption in each reaction was measured as the luciferase-derived luminescence by ARVO Light (PerkinElmer). At least three experiments were performed per condition and the averages and standard deviations of inhibition rates in each condition were evaluated to determine IC₅₀ values using the GraphPad Prism software.

4.3. Growth inhibition assay

A549, HCT-116 and MCF-7 cells were cultured in Dulbecco's modified Eagle's medium (DMEM, Sigma), McCoy's 5A medium (GIBCO) and Eagle's minimal essential medium (EMEM, Wako), respectively, supplemented with 10% (v/v) fetal bovine serum at 37 °C in a 5% CO₂-incubator. Growth inhibition assays using these cells were performed in 96-well plates (BD Falcon). A549, HCT-116 and MCF-7 cells were seeded at 500, 5000 and 5000 cells/well in 50 μ L of culture media, respectively, and were cultured for 6 h. Chemical compounds in DMSO were diluted 250-fold with the culture medium in advance. Following the addition of 40 μ L of the fresh culture medium to the cell cultures, 30 μ L of the chemical diluents were also added. The final volume of DMSO in the medium was equal to 0.1% (v/v). The cells under chemical treatment were incubated for further 72 h. The wells in the plates were washed twice with the cultured medium without phenol-red. After 1 h incubation with 100 μ L of the medium, the cell culture in each well was supplemented with 20 μ L of the MTS reagent (Promega), followed by incubation for additional 40 min. Absorbance at 490 nm of

each well was measured using a Wallac 1420 ARVO SX multilabel counter (Perkin Elmer). At least three experiments were performed per condition and the averages and standard deviations of inhibition rates in each condition were evaluated to determine IC₅₀ values using the GraphPad Prism software.

4.4. Thermodynamic solubility in aqueous solution

An equal volume of a mixture of 1/15 M phosphate buffer (pH 7.4, 0.5 mL) and EtOH (0.5 mL), or 1/15 M phosphate buffer (pH 7.4, 1.0 mL) was added to a compound in a vial. The suspension was then shaken for 48 h at 25 °C, and undissolved material was separated by filtration. *m*-Cresol was added as an internal standard (final concentration: 0.05 mg/mL) and the mixture was diluted in DMF and injected onto the HPLC column. The peak area ratio of the sample to the standard was recorded by UV detection at 254 nm. The concentration of the sample solution was calculated using a previously determined calibration curve, corrected for the dilution factor of the sample.

4.5. Molecular modeling

Docking calculations for compound **11d** were performed using a similar protocol in our previous research¹⁶ based on the crystal structure of the KSP-inhibitor complex (PDB ID: 3ZCW).²⁷ The protonation states of the amino acid residues of KSP and the direction of the hydrogen atoms involved in the hydrogen bonds were assigned using the Protonate3D algorithm²⁸ implemented in MOE.²⁹ The α 4/ α 6 allosteric site was chosen from the binding sites detected by the MOE-SiteFinder module. Docking pose generation was performed applying pharmacophore restraint to form hydrogen bonds with Asn271 and Leu292. The 100 initial docked candidate poses were optimized by the MMFF94x forcefield³⁰ and the pose with the lowest binding energy (E_{bind}) estimated by the MM/GBVI method³¹ was adopted as

the predicted binding mode.

Acknowledgements

This work was supported by Grants-in-Aid for Scientific Research, and Platform for Drug Discovery, Informatics, and Structural Life Science from MEXT, Japan. T. T. and R. M. are grateful for JSPS Research Fellowships for Young Scientists.

Supplementary data

Supplementary data associated with this article can be found, in the online version, at <http://dx.doi.org/10.1016/j.bmc.2014.04.008..>

References and notes

- 1 Miki, H.; Okada, Y.; Hirokawa, N. *Trends Cell Biol.* **2005**, *15*, 467.
- 2 Wordeman, L. *Semin. Cell Dev. Biol.* **2010**, *21*, 260.
- 3 Hirokawa, N.; Noda, Y.; Tanaka, Y.; Niwa, S. *Nat. Rev. Mol. Cell Biol.* **2009**, *10*, 682.
- 4 Kashina, A. S.; Baskin, R. J.; Cole, D. G.; Wedaman, K. P.; Saxton, W. M.; Scholey, J. M. *Nature* **1996**, *379*, 270.
- 5 Sawin, K. E.; LeGuellec, K.; Philippe, M.; Mitchison, T. J. *Nature* **1992**, *359*, 540.
- 6 Blangy, A.; Lane, H. A.; d'Herin, P.; Harper, M.; Kress, M.; Nigg, E. A. *Cell* **1995**, *83*, 1159.
- 7 Walczak, C. E.; Vernos, I.; Mitchison, T. J.; Karsenti, E.; Heald, R. *Curr. Biol.* **1998**, *8*, 903.
- 8 Mayer, T. U.; Kapoor, T. M.; Haggarty, S. J.; King, R. W.; Schreiber, S. L.; Mitchison, T. *J. Science* **1999**, *286*, 971.
- 9 Tao, W.; South, V. J.; Zhang, Y.; Davide, J. P.; Farrell, L.; Kohl, N. E.; Sepp-Lorenzino, L.; Lobell, R. B. *Cancer Cell.* **2005**, *8*, 49.
- 10 For a review, see: Jackson, J. R.; Patrick, D. R.; Dar, M. M.; Huang, P. S. *Nat. Rev. Cancer* **2007**, *7*, 107.
- 11 For a review, see: Matsuno, K.; Sawada, J.; Asai, A. *Expert Opin. Ther. Patent* **2008**, *18*, 253.
- 12 For a review, see: Sarli, V.; Giannis, A. *Clin. Cancer Res.* **2008**, *14*, 7583.
- 13 For a review, see: Rath, O.; Kozielski, F. *Nat. Rev. Cancer* **2012**, *12*, 527.
- 14 Oishi, S.; Watanabe, T.; Sawada, J.; Asai, A.; Ohno, H.; Fujii, N. *J. Med. Chem.* **2010**, *53*, 5054.
- 15 Takeuchi, T.; Oishi, S.; Watanabe, T.; Ohno, H.; Sawada, J.; Matsuno, K.; Asai, A.; Asada, N.; Kitaura, K.; Fujii, N. *J. Med. Chem.* **2011**, *54*, 4839.

- 16 Takeuchi, T.; Oishi, S.; Kaneda, M.; Ohno, H.; Nakamura, S.; Nakanishi, I.; Yamane, M.; Sawada, J.; Asai, A.; Fujii, N. *ACS Med. Chem. Lett.* doi: 10.1021/ml500016j
- 17 Yan, Y.; Sardana, V.; Xu, B.; Homnick, C.; Halczenko, W.; Buser, C. A.; Schaber, M.; Hartman, G. D.; Huber, H. E.; Kuo, L. C. *J. Mol. Biol.* **2004**, *335*, 547.
- 18 Kaan, H. Y. K.; Ulaganathan, V.; Hackney, D. D.; Kozielski, F. *Biochem. J.* **2010**, *425*, 55.
- 19 Barsanti, P. A.; Wang, W.; Ni, Z.; Duhl, D.; Brammeier, N.; Martin, E.; Bussiere, D.; Walter, A. O. *Bioorg. Med. Chem. Lett.* **2010**, *20*, 157.
- 20 For a recent review, see: Ishikawa, M.; Hashimoto, Y. *J. Med. Chem.* **2011**, *54*, 1539.
- 21 Anderson, K. W.; Tundel, R. E.; Ikawa, T.; Altman, R. A.; Buchwald, S. L. *Angew. Chem., Int. Ed.* **2006**, *45*, 6523.
- 22 Avdeef, A.; Testa, B. *Cell Mol. Life Sci.* **2002**, *59*, 1681.
- 23 Jalalian, N.; Ishikawa, E. E.; Silva, L. F., Jr.; Olofsson, B. *Org. Lett.* **2011**, *13*, 1552.
- 24 Kwong, F. Y.; Buchwald, S. L. *Org. Lett.* **2002**, *4*, 3517.
- 25 Cava, M. P.; Levinson, M. I. *Tetrahedron* **1985**, *41*, 5061.
- 26 The incompatible results between the in vitro KSP inhibition and cytotoxicity could be attributed to the varied cell membrane permeability. The less solubility of compound **13** in aqueous solution may be disadvantageous to the in vivo studies.
- 27 Ulaganathan, V.; Talapatra, S. K.; Rath, O.; Pannifer, A.; Hackney, D. D.; Kozielski, F. *J. Am. Chem. Soc.* **2013**, *135*, 2263.
- 28 Labute P. *Proteins*, **2009**, *75*, 187.
- 29 MOE ver 2010.10, Chemical Computing Group Inc., Montreal, Canada.
- 30 Halgren T. A.; Nachbar R. B. *J. Comput. Chem.*, **1996**, *17*, 587.
- 31 Labute P. *J. Comput. Chem.*, **2008**, *29*, 1693.

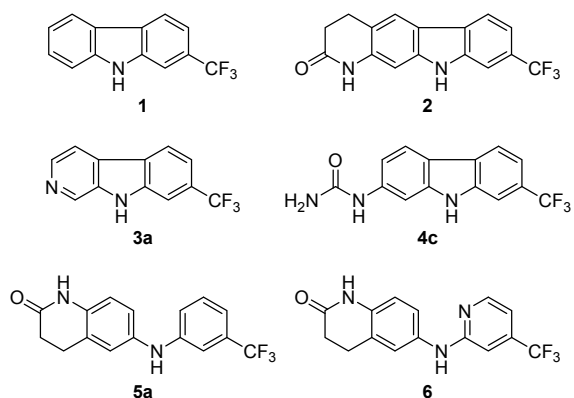


Figure 1. Structures of carbazole- and carboline-type (1–4) and diaryl amine-type (5, 6) KSP inhibitors.

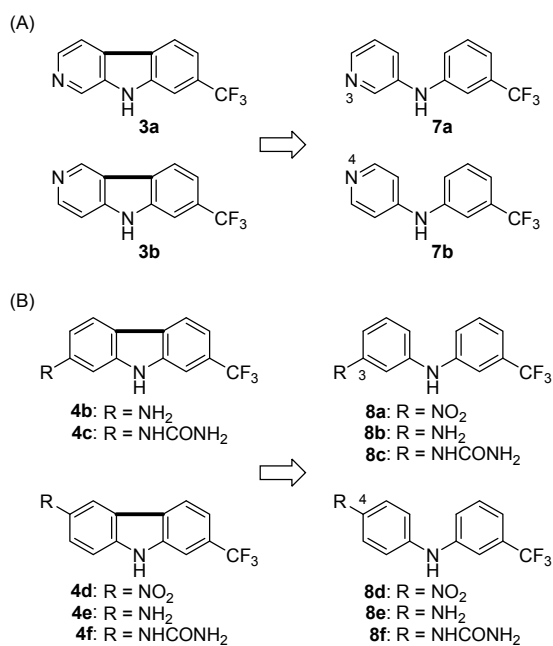


Figure 2. Design of novel KSP inhibitors **7**, **8** with diaryl amine scaffolds.

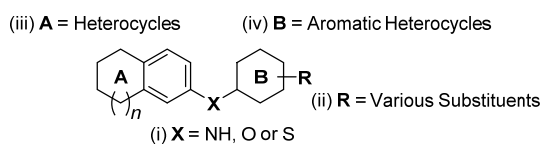


Figure 3. Strategy for the structure–activity relationship study of diaryl amine-type KSP inhibitors.

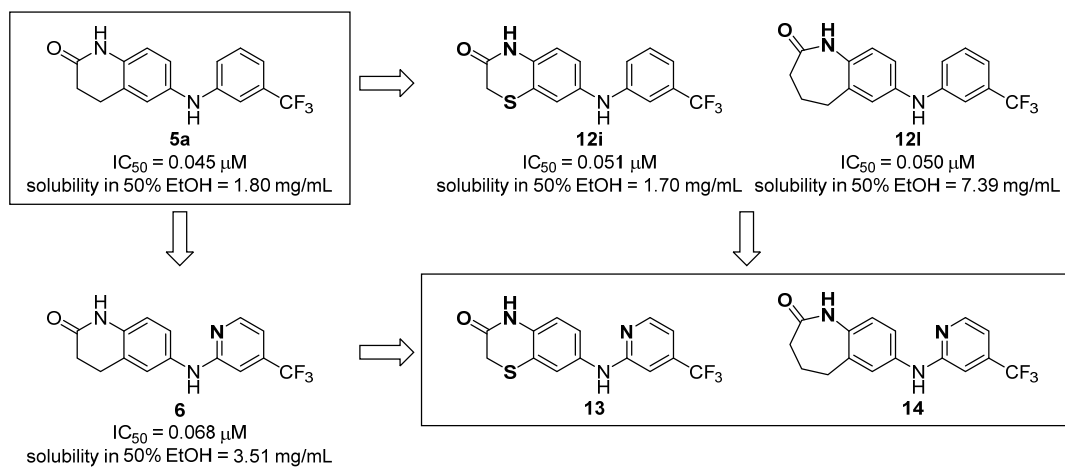


Figure 4. Design of novel diaryl amine-type KSP inhibitors **13** and **14**.

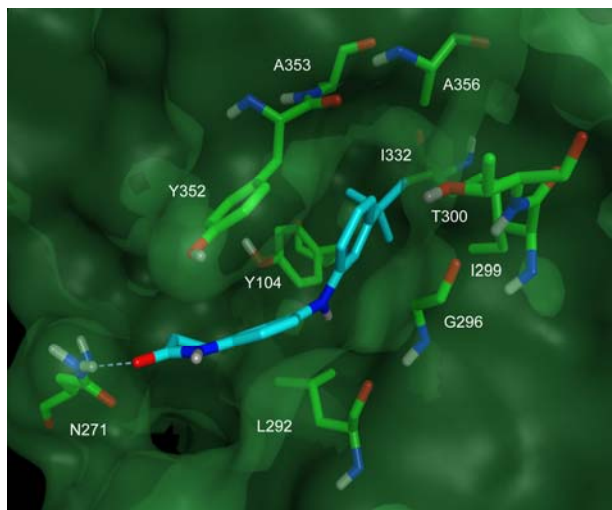
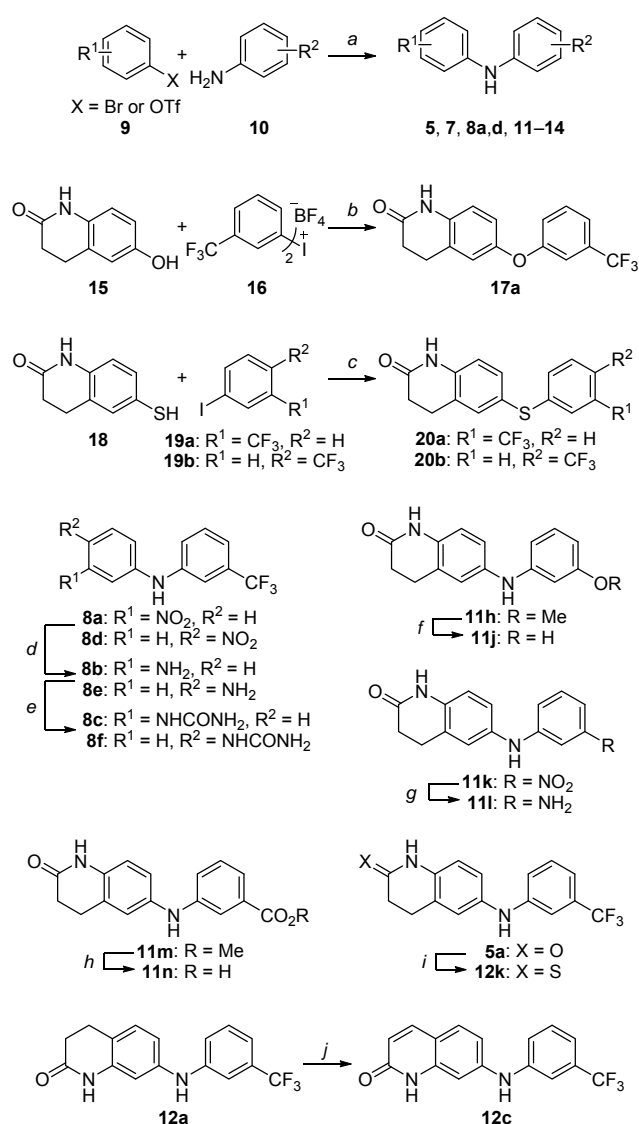
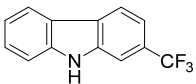
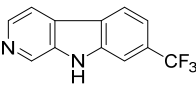
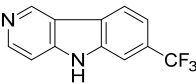
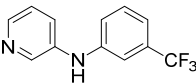
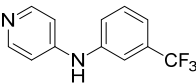


Figure 5. Plausible binding mode of diphenylamine **11d** at the interface of helices $\alpha 4$ and $\alpha 6$.



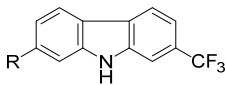
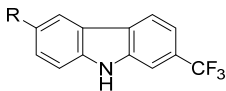
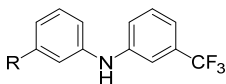
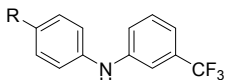
Scheme 1. Synthesis of diaryl amine derivatives. *Reagents and conditions:* (a) $\text{Pd}_2(\text{dba})_3$, biaryl phosphine ligand, NaOt-Bu , toluene, $100\text{ }^\circ\text{C}$; (b) KOt-Bu , DMF, $40\text{ }^\circ\text{C}$; (c) CuI , ethylene glycol, K_2CO_3 , 2-propanol, $80\text{ }^\circ\text{C}$; (d) Pd/C , HCO_2NH_4 , EtOH, reflux; (e) KOCN , AcOH, H_2O , rt; (f) BBr_3 , CH_2Cl_2 , rt; (g) Zn , AcOH, rt; (h) $\text{LiOH}\cdot\text{H}_2\text{O}$, MeOH, H_2O , $50\text{ }^\circ\text{C}$; (i) Lawesson's reagent, toluene, reflux; (j) $\text{Pd}(\text{OAc})_2$, O_2 , AcOH, $115\text{ }^\circ\text{C}$.

Table 1. KSP inhibitory activities and thermodynamic aqueous solubility of diaryl amines with a pyridine ring and the related compounds.

compound	KSP ATPase IC ₅₀ (μM) ^{a,b}	solubility	
		50% EtOH ^c (mg/mL)	phosphate buffer (pH 7.4) (μg/mL)
 1	0.21	0.424	<1
 3a	0.052	0.472	<1
 3b	0.095	1.76	3.16
 7a	>6.3 ^d	14.3	10.8
 7b	>6.3	24.0	264

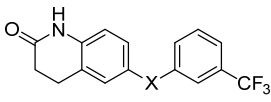
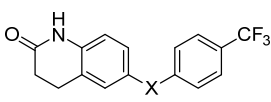
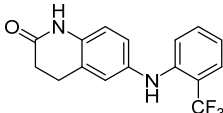
^aInhibition of microtubule-activated KSP ATPase activity. ^bIC₅₀ values were derived from the dose-response curves generated from triplicate data points. ^cSolubility in an equal volume of EtOH and 1/15 M phosphate buffer (pH 7.4). ^dIC₅₀ was ≈7.0 μM.

Table 2. KSP inhibitory activities of diphenylamines with a nitro, amino or urea group and the related carbazoles.

compound	R	KSP ATPase IC ₅₀ (μM) ^{a,b}
	4b NH ₂	0.27
	4c NHCONH ₂	0.085
	4d NO ₂	0.043
	4e NH ₂	0.55
	4f NHCONH ₂	0.12
	8a NO ₂	>6.3
	8b NH ₂	>6.3
	8c NHCONH ₂	>6.3
	8d NO ₂	3.2
	8e NH ₂	>6.3
	8f NHCONH ₂	0.39

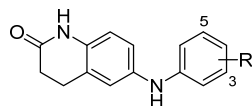
^aInhibition of microtubule-activated KSP ATPase activity. ^bIC₅₀ values were derived from the dose-response curves generated from triplicate data points.

Table 3. KSP inhibitory activities of dihydroquinolinone derivatives.

compound	X	KSP ATPase IC ₅₀ (μM) ^{a,b}
	5a NH	0.045
	17a O	2.0
	20a S	>6.3
	5b NH	0.33
	17b O	>6.3
	20b S	>6.3
	5c	>6.3

^aInhibition of microtubule-activated KSP ATPase activity. ^bIC₅₀ values were derived from the dose–response curves generated from triplicate data points.

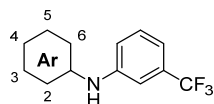
Table 4. KSP inhibitory activities of diphenylamines with a 3-substituent or 3,5-substituents on the right-hand phenyl group.



R		KSP ATPase IC ₅₀ (μM) ^{a,b}	R		KSP ATPase IC ₅₀ (μM) ^{a,b}
3-CF ₃	5a	0.045	3-OMe	11h	>6.3
H	11a	>6.3	3-OCF ₃	11i	1.2
3-Et	11b	0.81	3-OH	11j	>6.3
3- <i>i</i> -Pr	11c	0.43	3-NO ₂	11k	0.44
3- <i>t</i> -Bu	11d	0.16	3-NH ₂	11l	>6.3
3,5-di-CF ₃	11e	>6.3	3-CO ₂ Me	11m	>6.3
3-Ph	11f	>6.3	3-CO ₂ H	11n	>6.3
3-OPh	11g	>6.3			

^aInhibition of microtubule-activated KSP ATPase activity. ^bIC₅₀ values were derived from the dose–response curves generated from triplicate data points.

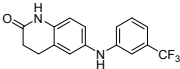
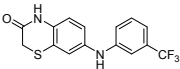
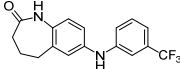
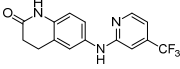
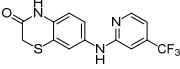
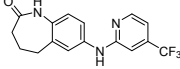
Table 5. KSP inhibitory activities of diphenylamines with a heterocycle on the left-hand phenyl group.



Ar	KSP ATPase IC ₅₀ (μM) ^{a,b}	Ar	KSP ATPase IC ₅₀ (μM) ^{a,b}
	5a 0.045		12h 0.29
	12a >6.3		12i 0.051
	12b >6.3		12j >6.3
	12c 4.6		12k 0.19
	12d >6.3		12l 0.050
	12e 3.6		12m 0.43
	12f >6.3		12n 0.92
	12g 0.81		

^aInhibition of microtubule-activated KSP ATPase activity. ^bIC₅₀ values were derived from the dose–response curves generated from triplicate data points.

Table 6. KSP inhibitory activities and physicochemical properties of diaryl amine derivatives **5a**, **6**, **12i**, **13** and **14**.

			
	5a	12i	12l
KSP ATPase IC ₅₀ (μM) ^{a,b}	0.045	0.051	0.050
Solubility in 50% EtOH (mg/mL) ^c	1.80	1.70	7.39
Solubility in phosphate buffer (pH 7.4) (μg/mL)	<1	<1	<1
melting point (°C)	190	166	140
ClogP ^d	4.2	4.0	4.4
HPLC retention time (min) ^e	24.4	28.2	27.0
			
	6	13	14
KSP ATPase IC ₅₀ (μM) ^{a,b}	0.068	0.035	0.050
Solubility in 50% EtOH (mg/mL) ^c	3.51	0.669	4.82
Solubility in phosphate buffer (pH 7.4) (μg/mL)	6.12	1.11	8.07
melting point (°C)	177	217	185
ClogP ^d	3.4	3.2	3.6
HPLC retention time (min) ^e	7.0	13.8	10.8

^aInhibition of microtubule-activated KSP ATPase activity. ^bIC₅₀ values were derived from the dose–response curves generated from triplicate data points. ^cSolubility in 50% EtOH [an equal volume of EtOH and 1/15 M phosphate buffer (pH 7.4)]. ^dClogP values were calculated with ChemBioDraw Ultra 12.0. ^eHPLC analysis was carried out on a Cosmosil 5C18-ARII column (4.6 × 250 mm) and the material eluted by a linear MeCN gradient (30-70% over 40 min) in 0.1% TFA; flow rate of 1 mL/min. ^aInhibition of microtubule-activated KSP ATPase activity. ^bIC₅₀ values were derived from the dose–response curves generated from triplicate data points. ^cSolubility in 50% EtOH [an equal volume of EtOH and 1/15 M phosphate buffer (pH 7.4)]. ^dClogP values were calculated with ChemBioDraw Ultra 12.0. ^eHPLC analysis was carried out on a Cosmosil 5C18-ARII column (4.6 × 250 mm) and the material eluted by a linear MeCN gradient (30-70% over 40 min) in 0.1% TFA; flow rate of 1 mL/min.

Table 7. Inhibitory effects on cell proliferation of diaryl amine-type KSP inhibitors toward A549, HCT-116 and MCF-7.

compound	IC ₅₀ (μM) ^a		
	A549	HCT-116	MCF-7
5a	4.2	8.9	11
6	2.5	4.4	8.0
12i	4.1	6.8	6.5
12l	4.5	5.7	3.9
13	1.5	2.6	2.8
14	5.0	6.5	9.1

^aIC₅₀ values were derived from the dose–response curves generated from triplicate data points.